HHS Public Access

Author manuscript

AJR Am J Roentgenol. Author manuscript; available in PMC 2015 April 01.

Published in final edited form as:

AJR Am J Roentgenol. 2011 November ; 197(5): W842–W851. doi:10.2214/AJR.11.6903.

Cardiac Masses, Part 2: Key Imaging Features for Diagnosis and Surgical Planning

Orla Buckley[1,2], **Rachna Madan**[1], **Raymond Kwong**[3], **Frank J. Rybicki**[4], and **Andetta Hunsaker**[1]

[1]Department of Radiology, Division of Thoracic Radiology, Brigham and Women's Hospital, Harvard Medical School, Boston, MA

[3]Division of Cardiology and Cardiac MRI, Brigham and Women's Hospital, Harvard Medical School, Boston, MA

[4]Department of Radiology, Noninvasive Imaging Laboratory, Brigham and Women's Hospital, Harvard Medical School, Boston, MA

Abstract

OBJECTIVE—The objectives of this article are to discuss key radiologic features that differentiate primary and secondary cardiac masses. Clinical scenarios are included to highlight stepwise radiologic workup of tumors of the pericardium, epicardium, myocardium, valves, and chambers. The involvement of key cardiac anatomic structures will also be emphasized to determine resectability and guide surgical planning.

CONCLUSION—Multimodality imaging plays a pivotal role in diagnosis and surgical planning of cardiac masses. Clinical features, such as patient age, location, and imaging characteristics of the mass will determine the likely differential diagnosis. In addition to radiologic evaluation of the mass itself, involvement of valvular apparatus, extent of myocardial involvement, or presence of associated coronary artery involvement is necessary to determine resectability and surgical technique.

Keywords

cardiac; cardiac CT; cardiac MRI; fibroma; myxoma; pericardium; thrombus

Introduction

In the case scenarios to follow, several examples of primary and secondary cardiac masses are described, including pericardial, myocardial, valvular, and subendocardial tumors.

Address correspondence to O. Buckley (orlabucko@gmail.com).

[2]Present address: Department of Radiology, Adelaide and Meath Hospital Incorporating the National Children's Hospital (AMCH), Tallaght, Dublin 24, Ireland.

SAM/CME

This article is available for SAM/CME credit. See www.arrs.org for more information.

WEB

This is a Web exclusive article.

Scenarios 1A and 1B

Clinical History of 1A

A 62-year-old man presented with a hypertensive crisis after colonoscopy (Fig. 1).

Clinical History of 1B

A 37-year-old woman with no medical history of cardiac disease presented with nausea, vomiting, headache, and hypertension (Fig. 2). A mass was detected in the atrioventricular groove on echocardiography, and urine catecholamines were elevated raising the suspicion of a pheochromocytoma.

Conclusion

The atrioventricular groove mass shown in Figure 1 is a pheochromocytoma (paraganglioma). The patient presented with clinical features of hypertensive crisis, which would be consistent with catecholamine excess. These masses are typically echogenic on echocardiography and on MRI they are T1 isointense or hypointense to myocardium, T2 hyperintense, and show avid enhancement after IV contrast administration [1].

Cardiac pheochromocytomas are typically 3–5 cm in size and found in an epicardial location in the roof of left atrium or anterior to the aortic root. Central necrosis is seen in 50% of cases, and calcifications are seen rarely [2]. At CT, cardiac paragangliomas are low attenuation on unenhanced imaging and after IV contrast administration enhance to the same degree as myocardium. Borders can be poorly defined as in this case (Fig. 1) [3]. Both octreotide and ^{131}I-metaiodobenzyl guanidine are used to detect pheochromocytomas and paragangliomas, with similar sensitivities of approximately 90% [2, 4]; ^{18}F-FDG avidity in paragangliomas is variable [5].

Surgical resection is the optimal management of cardiac paragangliomas. Preoperative tissue diagnosis can be obtained via catheterization or echocardiographic guidance. Preoperative percutaneous embolization of these tumors due to the increased vascularity has been described [6]. Cardiac bypass or cardiac autotransplantation may even be required because of the size of the tumor and complex anatomic relationship to the cardiac structures [7]. Paragangliomas anterior to the aortic root may necessitate aortic root replacement [7].

Coronary angiography in this patient with atrioventricular groove paraganglioma (Fig. 2) identified a patent but encased right coronary artery without evidence of ischemia distal to the site of involvement (no late gadolinium enhancement or regional wall motion abnormality in the right coronary artery perfusion territory). The patient underwent right coronary artery bypass grafting with saphenous vein graft from the aorta to the distal right coronary artery. MRI and echocardiography identified the tumor encroaching on the territory of the tricuspid annulus necessitating tricuspid valve replacement with a porcine valve. Because of the extent of pericardial and myocardial involvement, resection of the tumor necessitated patch replacement of the right atrial and right ventricular free wall with bovine pericardium. Preoperatively, identification of the length and depth of involvement of

the myocardium is necessary because, depending on the extent of involvement, a patch repair may or may not be feasible.

Scenario 2

Clinical History

A 46-year-old man presented with progressive shortness of breath and dizzy spells (Fig. 3).

Conclusion

The radiologic characteristics of this right atrial invasive mass with enhancement and flow voids are consistent with a right atrial angiosarcoma. Angiosarcoma is the most common primary cardiac malignant neoplasm in adulthood and typically occurs in middle-aged men [8]. Progressive dyspnea over months is the typical presentation [9]. Sarcomas occur typically in the right atrium with or without extension into the epicardial space and pericardium. Angiosarcomas may have a lobulated cauliflower configuration. These malignant tumors are typically isointense on T1-weighted MRI and hyperintense on T2-weighted MRI and show a heterogeneous enhancement pattern [10]. The heterogeneous enhancement is likely due to necrosis. The mass can show a characteristic sun-ray pattern because of diffuse intense enhancement [3]. Flow voids due to vascular structures within the mass may be present.

Scenarios 3A and 3B

Clinical History of 3A

A 63-year-old man with a history of prior coronary artery bypass grafting was found to have a left atrial mass at routine follow-up echocardiography (Fig. 4).

Clinical History of 3B

An 82-year-old man presented with atypical chest pain (Fig. 5).

Conclusion

Radiologic features of the mobile pedunculated left atrial mass arising from the interatrial septum (scenario 3A) were consistent with a myxoma. In scenario 3B, the location of the mass is atypical for a myxoma, but the pedunculated mobile enhancing mass structure raised the question of myxoma.

Cardiac myxomas typically occur in middle-aged adults (30–60 years) and in women more commonly than men [11–13]. Cardiac myxomas, the most common cardiac neoplasm in adulthood, are typically solitary and most commonly found in the left atrium (left atrium, 75%; right atrium, 25%) with the site of attachment most often adjacent to the fossa ovalis [14]. Myxomas are characteristically mobile, irregular, pedunculated masses that are isointense to myocardium on T1-weighted imaging, T2 hyperintense due to intracellular water, and have variable enhancement patterns. There may be hemorrhage within the myxoma, which will show variable signal intensity depending on chronicity [1, 10].

Although the stalk of the myxoma typically attaches to the interatrial septum at the border of the fossa ovalis, the tumor may originate from anywhere in the left atrium, including the atrial appendage. Myxomas have been reported to arise from the mitral valve apparatus [15], tricuspid valve, pulmonary artery and vein, and vena cava [16–18]. In a review of 49 patients with cardiac myxoma, 6.1% arose from the mitral valve [19]. When the mitral valve is involved, the mass may prolapse through the valve and may cause obstructive symptoms leading to life-threatening obstruction of the left ventricular outflow tract [15, 20].

Single atrial myxomas are generally sporadic, and the risk of recurrence is low after resection [21]. Multiplicity and right ventricular location are less commonly seen. Ventricular myxomas are more common in women and children and are often multiple; they typically arise from the free wall of the right ventricle and near the posterior papillary muscle of the left ventricle. Multiple tumors, atypical location of tumors, and recurrence after resection are seen in 7% of cases and are more common in younger men with a familial predisposition [21]. An example of such familial predisposition is the Carney complex, which consists of endocrinopathy; cardiac, cutaneous, and mammary myxomas; testicular neoplasm; LAMB (lentigines, atrial myxoma, mucocutaneous myxoma, and blue naevi); and NAME (naevi, atrial myxoma, myxoid neurofibroma, and ephilides) syndromes [22–25].

Indications for surgery include peripheral embolism, heart failure (mitral valve obstruction), right heart failure (right atrial tumor), and constitutional symptoms. Rarely, myxomas can undergo malignant degeneration [14]. Surgical resection of an atrial myxoma can involve a uniatrial or biatrial approach. Transaortic resection has also been used [20]. In many cases, resection from the valve is possible, rarely requiring valve replacement [26, 27]. A biatrial approach allows careful identification of the pedicle and prevention of perioperative embolization [28].

Scenario 4

Clinical History

A 76-year-old man with a history of lymphoma and atrial fibrillation was found to have a right atrial mass on echocardiography (Fig. 6). Twelve years previously the patient had undergone aortic valve replacement.

Conclusion

When thrombus may be the cause of an intracardiac mass, high-inversion-time (600–800 milliseconds) turbo FLASH single-shot magnitude images can be used to differentiate a thrombus from a mass [29]. The signal from thrombus is nulled at these high inversion times, and thus the thrombus becomes hypointense to myocardium. Thrombus will also fail to enhance with IV contrast administration. It is important to recognize that the signal isohyperintensity of the mass at an inversion time of 300 milliseconds does not represent vascularization of the mass but is due to the different null time of thrombus. This patient was at risk for both metastasis from known lymphoma and thrombus because of the known arrhythmia and the prosthetic valve. Therefore, this radiologic differentiation was crucial for guiding management.

Scenario 5

Clinical History

A 60-year-old man presented with near syncope (Fig. 7).

Conclusion

Lipomas are typically found in adults and can be found anywhere in the heart but are more commonly found in the epicardial region [9, 12]. Typically the tumors are slow growing and in the epicardial location can reach a large size and cause symptoms secondary to compression of the coronary arteries or can cause pericardial effusions [30]. Subendocardial lipomas are typically small and sessile and can cause obstructive symptoms [30]. Intramyocardial tumors can cause arrhythmias. Lipomatous hypertrophy of the interatrial septum is a benign condition commonly incidentally seen at echocardiography. Typically, this entity is identified as a nonenhancing smoothly marginated homogeneous dumbbell-shaped mass of fat attenuation that is confined to the interatrial septum [31]. On FDG PET/CT the maximum standardized uptake value of prominent lipomatous interatrial septal fat can be higher than that of the chest wall subcutaneous fat and can be mistaken for a mass [32] because of the presence of brown fat containing abundant mitochondria [33].

In this case, the tumor was large and the patient was symptomatic, requiring surgical resection of this mass. Despite being a benign tumor, the size of the mass necessitated resection of the right atrium and septum with reconstruction of the right anterior pulmonary veins, atrial septum, and right atrial wall with a bovine and autologous pericardial patch.

Scenario 6

Clinical History

A 77-year-old woman with shortness of breath on exertion was evaluated with echocardiography and found to a have a mass adherent to the aortic valve (Fig. 8).

Conclusion

The mass arising from the aortic valve is a fibroelastoma. The typical radiologic features of a fibroelastoma include a small pedunculated mass that is mobile with cardiac motion [9]. These are rare cardiac tumors but are among the more commonly seen benign cardiac tumors, most frequently in older adults (> 60 years) [9]. Fibroelastomas constitute 75% of all valvular tumors [34]. These tumors are found more commonly on the aortic and mitral valves but tricuspid and pulmonic valve fibroelastomas have been described [1, 34–38]. Typically, fibroclastomas are filiform projections measuring up to 1 cm which are found on the value leaflets or endocardial surface of the valve. Valvular function is not typically compromised by the lesion [34]. Often, these tumors are found incidentally because patients are frequently asymptomatic. The tumors are often seen on autopsy assessment of the valve or assessment of the valve after resection. Although histologically benign, these tumors can cause systemic embolization, resulting in stroke or embolization into the coronary arteries causing chest pain or myocardial infarction [39, 40].

Lambl excrescences are filiform fronds originating at sites of valve closure, unlike fibroelastomas that occur anywhere on the valve [40]. In the echocardiographic literature, these are often referred to as valvular strands [41, 42]. They are also associated with surface thrombi, and patients may experience embolic events and hence anticoagulation may be needed [41]. Differentiation between fibroelastoma, thrombus, and vegetations can be difficult.

Fibroelastomas are resected if the tumor is mobile or pedunculated and prolapses into the valve or outflow tract, if it is seen to grow, or if it is symptomatic. If patients are undergoing cardiac surgery for any other reason, the mass may also be resected at the same time. Typically, valve sparing surgery is feasible [43], although sometimes leaflet reconstruction with a pericardial patch may be required [43, 44]. Recurrence is rare [9, 45].

Most fibroelastomas are successfully resected without the need for valve repair, as was the case in this patient. If there is concomitant valve degeneration, valve repair is often considered at the time of resection.

Scenario 7

Clinical History

A 47-year-old woman presented with shortness of breath. Echocardiography showed a pericardial effusion that was drained and sent for microbiology and cytologic analysis. Four months later, the patient presented with increasing shortness of breath and underwent cardiac CT and cardiac MRI (Fig. 9). She had no skin lesions, and her complete blood count was normal. Mammography and breast examination findings were normal. Her lung parenchyma was normal with no focal lesions.

Conclusion

Cytologic analysis of the pericardial effusion was consistent with primary pericardial mesothelioma. Primary pericardial mesothelioma is the most common primary malignant pericardial tumor [46]. Mesothelioma may involve the pleura in 88.8%, peritoneum in 9.6%, and pericardium in 0.7% of cases [46, 47]. This is a rare tumor of the pericardium, occurring in 0.0022% of patients and in 1% of patients with mesothelioma [46, 47]. This tumor typically presents with pericardial effusion and nodular pericardial thickening with or without plaques. Debulking of the tumor was considered, but the involvement of the left anterior descending artery as well as the right coronary artery (seen on other images) indicated the tumor was unresectable. Primary pericardial malignancy is rare but can be due to mesothelioma, lymphoma, sarcoma, or liposarcoma. In cases of primary pericardial mesothelioma, pericardial nodules or calcified plaque may be present. There can also be direct secondary invasion of the pericardium by pleural-based mesothelioma.

Pericardial metastases are more common than primary pericardial tumors, most commonly from breast or lung primaries via lymphatic, hematogenous, or direct spread [35, 48–50]. Lymphoma and melanoma are also known to have a predilection for pericardial spread [50, 51].

Radiologically, the presence of a pericardial effusion with masslike or nodular enhancing pericardial thickening that obliterates the epicardial fat planes is concerning for malignancy, but the differential diagnosis for pericardial thickening with pericardial effusion includes benign and malignant causes. Malignant pericardial effusions can typically be hemorrhagic and loculated. Identification of involvement of the epicardial fat or myocardium will determine whether pericardectomy may be possible. The optimal strategy to make this determination is using cardiac MRI with double inversion recovery sequences, most helpful because of high spatial and contrast resolution.

Benign causes of pericarditis typically result in smooth pericardial thickening and pericardial effusion and include sarcoidosis, rheumatoid arthritis, uremia, or radiation-induced pericarditis [51]. Tuberculous pericarditis can, however, mimic pericardial malignancy because it can be associated with nodular pericardial thickening.

Scenario 8

Clinical History

A 23-year-old man with a history of shortness of breath and back pain was found to have a pericardial mass that was biopsy-proven to represent epithelioid mesothelioma (Fig. 10). Cardiac MRI was performed to determine whether there was invasion of the epicardial space and left ventricular myocardium.

Conclusion

In cases of tumor abutting the pericardium with suspected infiltration of the epicardial fat and myocardium, double inversion recovery images provide high contrast and spatial resolution imaging of the tissue planes. Where tissue planes are obliterated, dynamic imaging with steady-state free precession tagged sequences can help to determine the presence of myocardial adhesions or infiltration.

Scenario 9

Clinical History

A 42-year-old woman presented with progressive shortness of breath and atypical chest pain (Fig. 11).

Conclusion

This mass was histologically consistent with fibroma, a tumor that is more commonly seen in the pediatric population [9, 12, 50, 51]. It is usually solitary and occurs in the interventricular septum or left ventricular free wall [3]. Fibromas can be well or poorly defined [34]. Atrial location is more commonly seen in patients with polyposis syndromes such as Gardner syndrome [9, 35]. Focal calcifications may be present. The presence of calcifications helps differentiation of fibromas from rhabdomyomas, which do not show calcification [9, 35]. The tumor is typically in the region of 5 cm at diagnosis (range of 2–10 cm) [3, 9]. MR characteristics of fibromas include iso- or hypointensity to the myocardium on T1- and T2-weighted sequences because of their dense fibrous nature. In contrast,

rhabdomyomas are isointense on T1-weighted imaging and hyperintense on T2-weighted imaging [9]. Fibromas frequently show moderate to intense enhancement [10], but the enhancement pattern is variable [3, 35].

Rhabdomyomas are typically multiple and arise more frequently in the ventricles than the atria. On T1-weighted images, they are typically isointense with myocardium and iso- to hyperintense on T2-weighted images. The enhancement pattern is variable [9, 35]. When small diffuse intramyocardial lesions are present, diffuse myocardial thickening may be the predominant feature on echocardiography [50]. Contrast-enhanced MRI can be used to better define the borders of these tumors.

Fibromas are the most common surgically resected primary cardiac tumor in childhood. Surgical removal with enucleation is successful in some patients, but complete resection is not always possible, depending on the degree of myocardium involvement and involvement of critical structures, such as papillary muscles or the conduction system. In this patient, surgical resection necessitated mitral valve repair because of involvement of the papillary muscles.

Rhabdomyomas are typically discovered in the neonatal period. These are frequently associated with tuberous sclerosis (seen in 50% of patients with tuberous sclerosis), although they can occur sporadically. Because spontaneous regression of rhabdomyomas is commonly observed, surgical resection is not frequently indicated. If there is outflow tract obstruction or arrhythmia, surgical resection may be required [14, 35, 51].

Scenario 10

Clinical History

A 69-year-old man with a history of melanoma with incidental discovery of an atrioventricular groove mass on echocardiography (Fig. 12).

Conclusion

Malignant melanoma can metastasize to the heart and is most commonly found in the epicardial regions [52, 53]. Cardiac metastases from melanoma primary tumors are identified in 2% of patients but at autopsy are found in as high as 50% of patients [53]. Because of the melanin content, melanoma metastases are typically hyperintense on T1-weighted imaging and will enhance after contrast administration. The extent of T1 hyperintensity is dependent on the amount of melanin in the lesion. Melanoma metastases are prone to hemorrhage; the presence of methemoglobin can also cause T1 shortening [14].

The most common site of metastasis to the heart is the epicardium, followed by the pericardium and myocardium [48]. Endocardial metastases are rare but are more commonly seen in renal cell cancer, hepatocellular cancer, or melanoma and typically involve the right heart [3]. The most common pathway for tumor spread to the heart is via retrograde flow of tumor cells through the lymphatic system to the epicardium or via hematogenous spread, typically to the myocardium.

Scenario 11

Clinical History

A 65-year-old man presented with a mass and pain in the right shoulder region found to be secondary to a fibromyxoid sarcoma of the scapula on imaging. He underwent serial resections and subsequent right forequarter amputation. Follow-up CT over a 9-month period is shown in Figures 13A–13C. Figure 13A was obtained at presentation with symptoms of shortness of breath; 13B, was obtained at 3 months after presentation; and 13C was obtained at 9 months after presentation. Axial T1 unenhanced (Fig 13C) and contrast-enhanced (Fig. 13E) cardiac MR images were obtained to characterize the extent of thrombus versus true mass. The resected pathologic specimen is shown in Figure 13F.

Conclusion

The patient had a fibromyxoid tumor of the scapula and underwent right forequarter amputation. When the masslike filling defect was seen progressively extending from the right subclavian vein toward the right heart, radiologic differentiation of the extent of thrombus versus tumor was necessary. The key diagnostic feature was whether the mass showed enhancement with contrast administration; a solid tumor would be expected to enhance whereas thrombus would not. Differentiating between thrombus and tumor could be possible on CT if unenhanced and contrast-enhanced images had been provided to determine whether enhancement was present. On the late gadolinium-enhanced image shown in Figure 13A, there is enhancement of the mass in the heart with peripheral rim of non-enhancement. Preoperatively, it was suspected that this represented a solid tumor with a rim of thrombus at its surface, which was confirmed surgically and histologically.

Leiomyosarcoma is a malignant tumor of smooth muscle and often arises in the pulmonary vasculature spreading into the left atrium [3]. These tumors are lobulated masses in the left atrium that can be differentiated from left atrial myxomas by location and invasiveness. Typically, leiomyosarcomas arise from the posterior wall in the region of the pulmonary venous confluences as opposed to myxomas, which arise in the region of the interatrial septum. These tumors can be aggressive, and invasion of the pulmonic veins or mitral valve can occur [1].

Transvenous spread of tumors is less common and typically seen from tumors extending from the infrarenal inferior vena cava. Right atrial extension of subdiaphragmatic tumors can be seen, especially with renal cancers as well as hepatic, adrenal, and uterine cancers. Ten percent of renal cell cancers invade the inferior vena cava, of which up to 40% spread to the heart [54]. Extension of tumor along the superior vena cava is rare. Lung cancers can spread by direct invasion, transvenous spread through the pulmonary vein, and retrograde lymphangitic spread.

Supplementary Material

Refer to Web version on PubMed Central for supplementary material.

References

1. Araoz PA, Mulvagh SL, Tazelaar HD, Julsrud PR, Breen JF. CT and MR imaging of benign primary cardiac neoplasms with echocardiographic correlation. RadioGraphics. 2000; 20:1303–1319. [PubMed: 10992020]
2. Hamilton BH, Francis IR, Gross BH, et al. Intra-pericardial paragangliomas (pheochromocytomas): imaging features. AJR. 1997; 168:109–113. [PubMed: 8976931]
3. O'Sullivan PJ, Gladish GW. Cardiac tumors. Semin Roentgenol. 2008; 43:223–233. [PubMed: 18486683]
4. Colwell AS, D'Cunha J, Maddaus MA. Carney's triad paragangliomas. J Thorac Cardiovasc Surg. 2001; 121:1011–1012. [PubMed: 11326257]
5. Fukuchi K, Inenaga T, Suzuki Y, Horita Y, Hayashida K, Ishida Y. Paraganglioma seen with FDG dual-head gamma camera coincidence imaging after false-negative results of I-123 MIBG imaging. Clin Nucl Med. 2001; 26:966–967. [PubMed: 11595866]
6. Rakovich G, Ferraro P, Therasse E, Duranceau A. Preoperative embolization in the management of a mediastinal paraganglioma. Ann Thorac Surg. 2001; 72:601–603. [PubMed: 11515906]
7. Yendamuri S, Elfar M, Walkes JC, Reardon MJ. Aortic paraganglioma requiring resection and replacement of the aortic root. Interact Cardiovasc Thorac Surg. 2007; 6:830–831. [PubMed: 17901107]
8. Burke AP, Cowan D, Virmani R. Primary sarcomas of the heart. Cancer. 1992; 69:387–395. [PubMed: 1728367]
9. Grebenc ML, Rosado de Christenson ML, Burke AP, Green CE, Galvin JR. Primary cardiac and pericardial neoplasms: radiologic-pathologic correlation. RadioGraphics. 2000; 20:1073–1103. quiz, 1110–1112. [PubMed: 10903697]
10. Kaminaga T, Takeshita T, Kimura I. Role of magnetic resonance imaging for evaluation of tumors in the cardiac region. Eur Radiol. 2003; 13(suppl 6):L1–L10.
11. Pinede L, Duhaut P, Loire R. Clinical presentation of left atrial cardiac myxoma: a series of 112 consecutive cases. Medicine (Baltimore). 2001; 80:159–172. [PubMed: 11388092]
12. Butany J, Nair V, Naseemuddin A, Nair GM, Catton C, Yau T. Cardiac tumours: diagnosis and management. Lancet Oncol. 2005; 6:219–228. [PubMed: 15811617]
13. Arciniegas E, Hakimi M, Farooki ZQ, Truccone NJ, Green EW. Primary cardiac tumors in children. J Thorac Cardiovasc Surg. 1980; 79:582–591. [PubMed: 7359937]
14. Sparrow PJ, Kurian JB, Jones TR, Sivananthan MU. MR imaging of cardiac tumors. RadioGraphics. 2005; 25:1255–1276. [PubMed: 16160110]
15. Keeling I, Oberwalder P, Schuchlenz H, Anelli-Monti M, Rigler B. Left ventricular outflow tract obstruction due to valve myxoma. Ann Thorac Surg. 2000; 69:1590–1591. [PubMed: 10881855]
16. McAllister HA Jr. Primary tumors of the heart and pericardium. Pathol Annu. 1979; 14:325–355. [PubMed: 232754]
17. Jones DR, Hill RC, Abbott AE Jr, Gustafson RA, Murray GF. Unusual location of an atrial myxoma complicated by a secundum atrial septal defect. Ann Thorac Surg. 1993; 55:1252–1253. [PubMed: 8494444]
18. Yuan SM, Shinfeld A, Raanani E. Tricuspid valve myxoma: a case report and a collective review of the literature. J Card Surg. 2009; 24:69–72. [PubMed: 19120679]
19. Keeling IM, Oberwalder P, Anelli-Monti M, et al. Cardiac myxomas: 24 years of experience in 49 patients. Eur J Cardiothorac Surg. 2002; 22:971–977. [PubMed: 12467822]
20. Keeling I, Oberwalder PJ, Rigler B. Transaortic access for excision of a left ventricular myxoma. Ann Thorac Surg. 1999; 68:2384–2385. [PubMed: 10617051]
21. Grebenc ML, Rosado-de-Christenson ML, Green CE, Burke AP, Galvin JR. Cardiac myxoma: imaging features in 83 patients. RadioGraphics. 2002; 22:673–689. [PubMed: 12006696]
22. Yin Z, Kirschner LS. The Carney complex gene *PRKAR1A* plays an essential role in cardiac development and myxomagenesis. Trends Cardiovasc Med. 2009; 19:44–49. [PubMed: 19577711]

23. Vargas-Alarcon G, Vargas-Barron J, Cruz-Robles D, et al. A deletion in the *PRKAR1A* gene is associated with Carney complex. J Pediatr Endocrinol Metab. 2008; 21:705–709. [PubMed: 18780607]
24. Vidaillet HJ Jr, Seward JB, Fyke E 3rd, Tajik AJ. NAME syndrome (nevi, atrial myxoma, myxoid neurofibroma, ephelides): a new and unrecognized subset of patients with cardiac myxoma. Minn Med. 1984; 67:695–696. [PubMed: 6513916]
25. Rhodes AR, Silverman RA, Harrist TJ, Perez-Atayde AR. Mucocutaneous lentigines, cardiomucocutaneous myxomas, and multiple blue nevi: the “LAMB” syndrome. J Am Acad Dermatol. 1984; 10:72–82. [PubMed: 6693605]
26. Gunther T, Schreiber C, Noebauer C, Eicken A, Lange R. Treatment strategies for pediatric patients with primary cardiac and pericardial tumors: a 30-year review. Pediatr Cardiol. 2008; 29:1071–1076. [PubMed: 18600370]
27. Kabbani SS, Cooley DA. Atrial myxoma: surgical considerations. J Thorac Cardiovasc Surg. 1973; 65:731–737. [PubMed: 4696873]
28. Kabbani SS, Jokhadar M, Meada R, et al. Atrial myxoma: report of 24 operations using the biatrial approach. Ann Thorac Surg. 1994; 58:483–487. discussion, 487–488. [PubMed: 8067852]
29. Barkhausen J, Hunold P, Eggebrecht H, et al. Detection and characterization of intracardiac thrombi on MR imaging. AJR. 2002; 179:1539–1544. [PubMed: 12438051]
30. Gaerte SC, Meyer CA, Winer-Muram HT, Tarver RD, Conces DJ Jr. Fat-containing lesions of the chest. RadioGraphics. 2002; 22(spec):S61–S78. [PubMed: 12376601]
31. Meaney JF, Kazerooni EA, Jamadar DA, Korobkin M. CT appearance of lipomatous hypertrophy of the interatrial septum. AJR. 1997; 168:1081–1084. [PubMed: 9124119]
32. Kuester LB, Fischman AJ, Fan CM, Halpern EF, Aquino SL. Lipomatous hypertrophy of the interatrial septum: prevalence and features on fusion ^{18}F fluorodeoxyglucose positron emission tomography/CT. Chest. 2005; 128:3888–3893. [PubMed: 16354859]
33. Shammas A, Lim R, Charron M. Pediatric FDG PET/CT: physiologic uptake, normal variants, and benign conditions. RadioGraphics. 2009; 29:1467–1486. [PubMed: 19755606]
34. Kim EY, Choe YH, Sung K, Park SW, Kim JH, Ko YH. Multidetector CT and MR imaging of cardiac tumors. Korean J Radiol. 2009; 10:164–175. [PubMed: 19270863]
35. O’Donnell DH, Abbara S, Chaithiraphan V, et al. Cardiac tumors: optimal cardiac MR sequences and spectrum of imaging appearances. AJR. 2009; 193:377–387. [PubMed: 19620434]
36. Edwards WD. Pulmonary embolization of papillary fibroelastoma arising from the tricuspid valve. Tex Heart Inst J. 1991; 18:226–227. [PubMed: 15227486]
37. Klarich KW, Enriquez-Sarano M, Gura GM, Edwards WD, Tajik AJ, Seward JB. Papillary fibroelastoma: echocardiographic characteristics for diagnosis and pathologic correlation. J Am Coll Cardiol. 1997; 30:784–790. [PubMed: 9283541]
38. Khair T, Mazidi P, Laos LF. Cardiac papillary fibroelastoma: case report and review of the literature. Int J Cardiol. 2010; 139:102–104. [PubMed: 18718682]
39. DiLorenzo WR, Donohue TJ, Ghantous AE. Papillary fibroelastoma arising from the pulmonary valve associated with pulmonary embolization. Conn Med. 2008; 72:143–146. [PubMed: 18426180]
40. Alessi A, Gomes de Carvalho R, Bertolin Precoma D, et al. Fibroelastoma of the mitral valve as a cause of transient ischemic stroke. Arq Bras Cardiol. 2001; 77:77–84. [PubMed: 11500751]
41. Aziz F, Baciewicz FA Jr. Lambl’s excrescences: review and recommendations. Tex Heart Inst J. 2007; 34:366–368. [PubMed: 17948090]
42. Jaffe W, Figueredo VM. An example of Lambl’s excrescences by transesophageal echocardiogram: a commonly misinterpreted lesion. Echocardiography. 2007; 24:1086–1089. [PubMed: 18001363]
43. Gopaldas RR, Atluri PV, Blaustein AS, Bakaeen FG, Huh J, Chu D. Papillary fibroelastoma of the aortic valve: operative approaches upon incidental discovery. Tex Heart Inst J. 2009; 36:160–163. [PubMed: 19436815]
44. Westhof FB, Chryssagis K, Liangos A, Batz G, Diegeler A. Aortic valve leaflet reconstruction after excision of a papillary fibroelastoma using autologous pericardium. Thorac Cardiovasc Surg. 2007; 55:204–207. [PubMed: 17410513]

45. Ngaage DL, Mullany CJ, Daly RC, et al. Surgical treatment of cardiac papillary fibroelastoma: a single center experience with eighty-eight patients. Ann Thorac Surg. 2005; 80:1712–1718. [PubMed: 16242444]
46. Kainuma S, Masai T, Yamauchi T, Takeda K, Ito H, Sawa Y. Primary malignant pericardial mesothelioma presenting as pericardial constriction. Ann Thorac Cardiovasc Surg. 2008; 14:396–398. [PubMed: 19131929]
47. Hillerdal G. Malignant mesothelioma 1982: review of 4710 published cases. Br J Dis Chest. 1983; 77:321–343. [PubMed: 6357260]
48. Chiles C, Woodard PK, Gutierrez FR, Link KM. Metastatic involvement of the heart and pericardium: CT and MR imaging. RadioGraphics. 2001; 21:439–449. [PubMed: 11259706]
49. Wang ZJ, Reddy GP, Gotway MB, Yeh BM, Hetts SW, Higgins CB. CT and MR imaging of pericardial disease. RadioGraphics. 2003; 23(spec):S167–S180. [PubMed: 14557510]
50. Coates TL, McGahan JP. Fetal cardiac rhabdomyomas presenting as diffuse myocardial thickening. J Ultrasound Med. 1994; 13:813–816. [PubMed: 7823347]
51. Beghetti M, Gow RM, Haney I, Mawson J, Williams WG, Freedom RM. Pediatric primary benign cardiac tumors: a 15-year review. Am Heart J. 1997; 134:1107–1114. [PubMed: 9424072]
52. Tesolin M, Lapierre C, Oligny L, Bigras JL, Champagne M. Cardiac metastases from melanoma. RadioGraphics. 2005; 25:249–253. [PubMed: 15653599]
53. Glancy DL, Roberts WC. The heart in malignant melanoma: a study of 70 autopsy cases. Am J Cardiol. 1968; 21:555–571. [PubMed: 5650736]
54. Prager RL, Dean R, Turner B. Surgical approach to intracardiac renal cell carcinoma. Ann Thorac Surg. 1982; 33:74–77. [PubMed: 7065766]

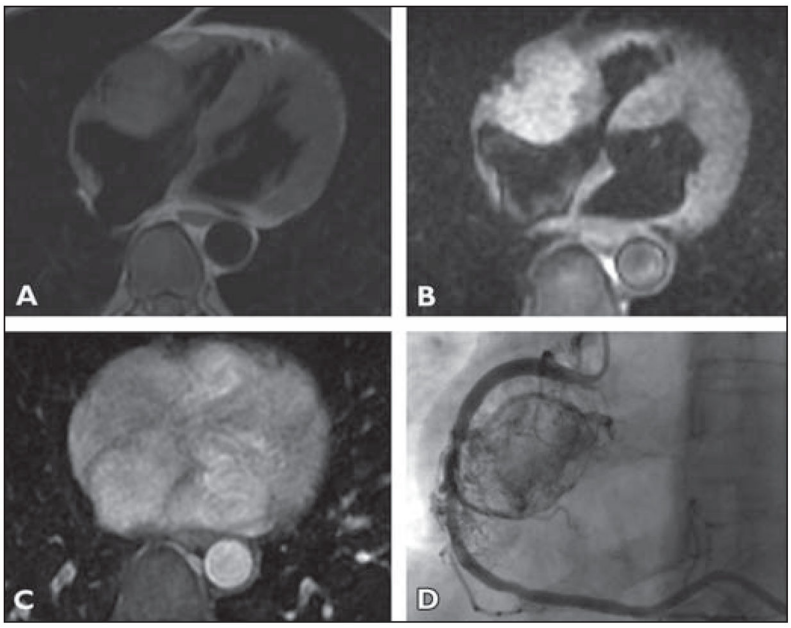

Fig 1. 62-year-old man who presented with hypertensive crisis after colonoscopy

A, T1-weighted image (**A**) shows round mass in right atrioventricular groove that is isointense to myocardium. On T2-weighted image (**B**), mass is hyperintense to myocardium.

C, Axial postcontrast T1-weighted image with fat saturation shows homogeneous enhancement of the mass.

D, Coronary angiogram with selective catheterization and injection of right coronary artery (RCA) shows highly vascular mass receiving perfusion from RCA. In its mid section, RCA has lost its normal smooth contour and invasion-encasement by tumor is suspected. For dynamic cine images from angiography, see Figure S1, cine loop, in supplemental data online.

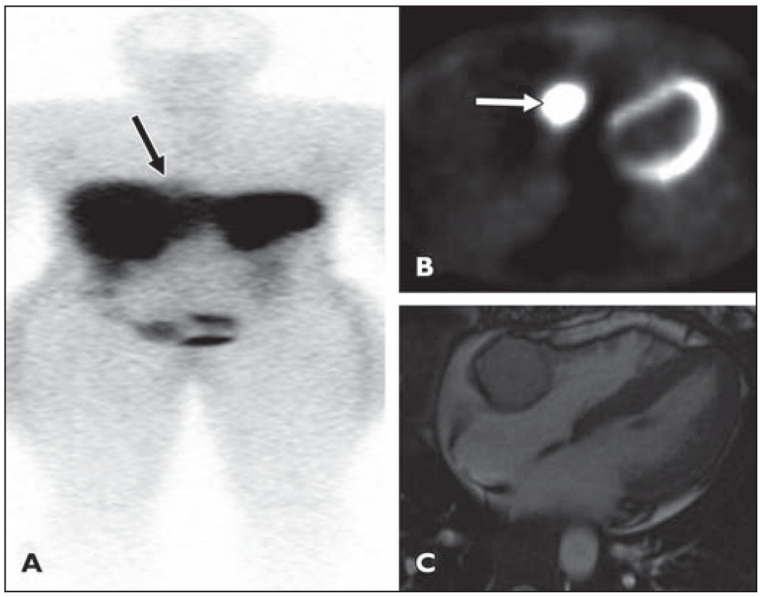

Fig 2.

37-year-old woman with no history of cardiac disease who presented with nausea, vomiting, headache, and hypertension. Mass was detected in atrioventricular groove on echocardiography and urine catecholamines were elevated, raising suspicion of pheochromocytoma. See Figure S2, cine loop, in supplemental data online.

A, After injection of 5.8 mCi of ^{111}In octreotide, faint focus of tracer accumulation (*arrow*), better seen on anterior planar images, is noted in medial right hemithorax adjacent to diaphragm in region of right anterior mediastinum.

B, Image shows mass is ^{18}F-FDG avid (*arrow*).

C, Cardiac MR image confirms well-defined lobular mass in right atrioventricular groove, lying between right coronary artery and myocardium.

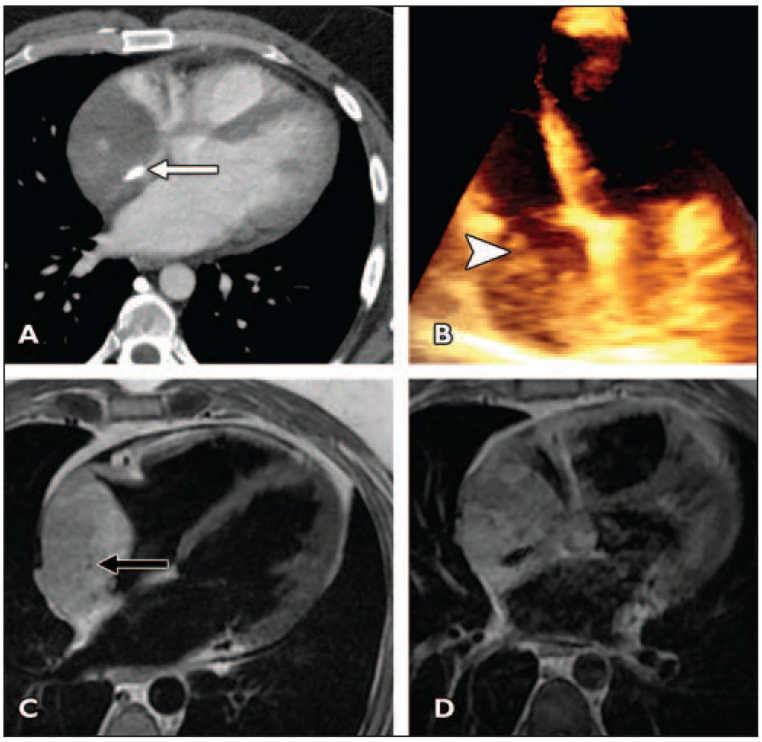

Fig 3. 46-year-old man who presented with progressive shortness of breath and dizzy spells

A, Axial contrast-enhanced CT image shows enhancing irregular mass containing focal coarse calcification (*arrow*).

B, 3D echocardiogram confirms lobulated right atrial mass (*arrowhead*). Mass does not involve tricuspid apparatus or reach interatrial septum.

C, T1-weighted double inversion recovery image confirms mass is mildly hyperintense to myocardium, and punctate flow voids are seen in mass (*arrow*), corresponding to vascular structures.

D, Contrast-enhanced T1-weighted fat-saturated double inversion recovery image shows mass enhances inhomogeneously. Focal calcification is seen as ovoid signal void.

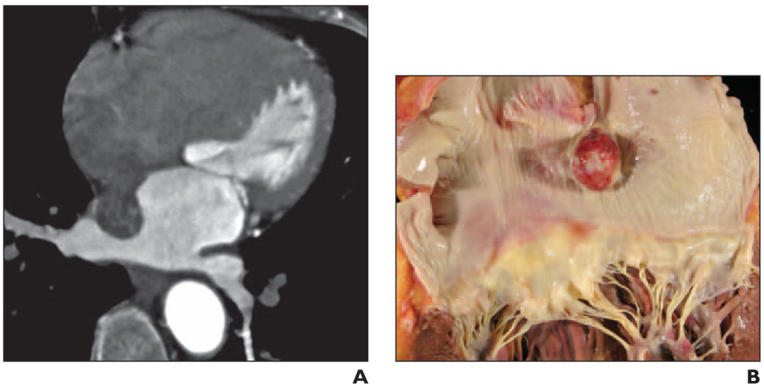

Fig 4. 63-year-old man with history of coronary artery bypass grafting who was found to have left atrial mass at routine follow-up echocardiography

A, Axial gated cardiac CT image (acquired after administration of 75 mL of nonionic contrast material (370 mmol/kg) followed by 40 mL of saline administered at 5 mL/s) with corresponding dynamic CT (see Figure S4A, cine loop, in supplemental data online) shows well-defined mobile round mass in left atrium adherent to interatrial septum via thin pedicle. Dynamic cardiac CT images were acquired using single heartbeat acquisition 320-MDCT with 0.6-mm spatial resolution and temporal resolution of 175 milliseconds. Tube current modulation was used to reduce radiation exposure but allow data recovery from full R-R interval.

B, Gross pathology image of resected specimen shows smooth round mass arising from interatrial septum, consistent with myxoma.

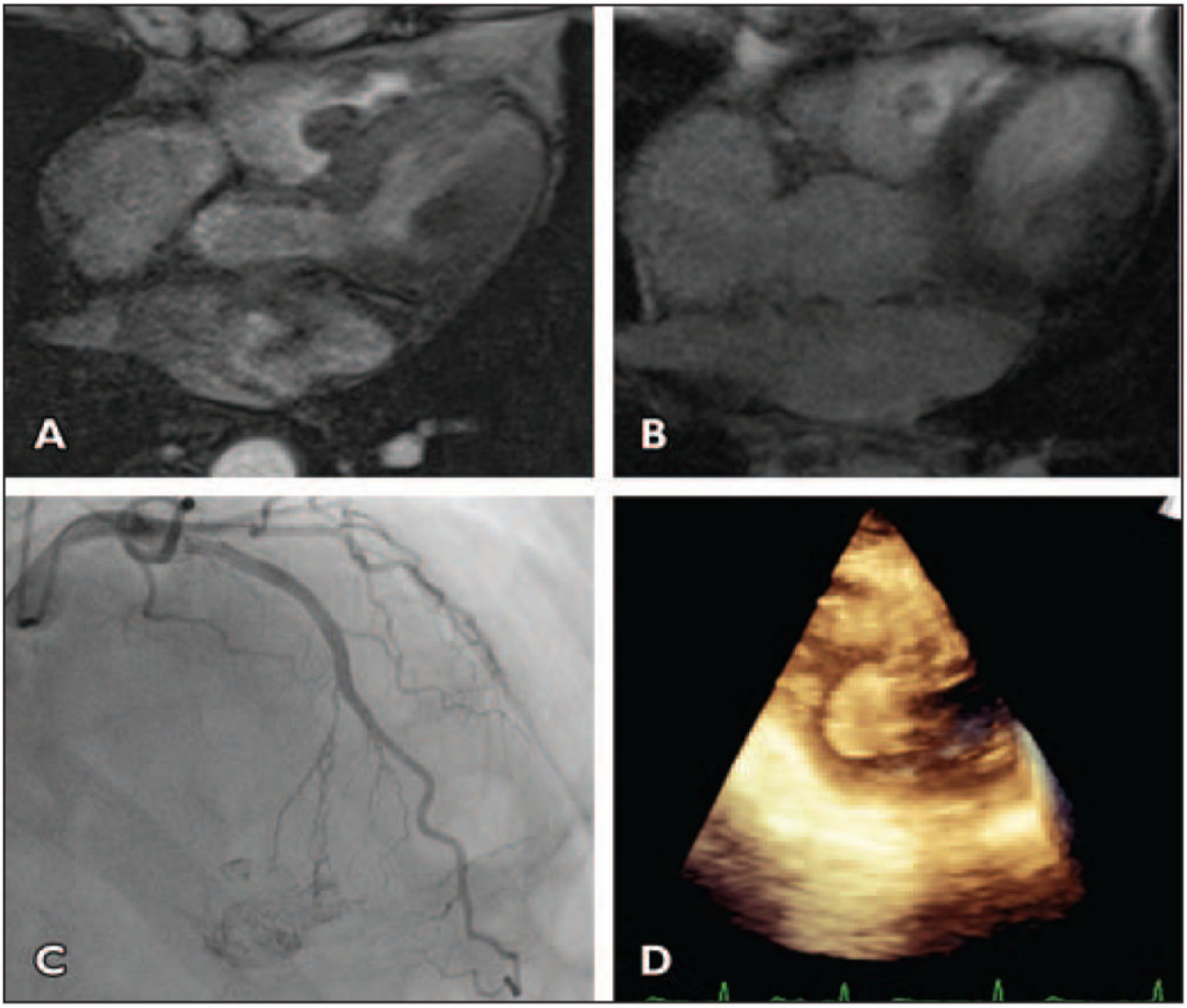

Fig 5. 82-year-old man with atypical chest pain

A, Axial gradient-echo CT image shows round pedunculated mass arising from interventricular septum in basal right ventricle. See Figure S5A, cine loop, in supplemental data online.

B, Axial postcontrast T1-weighted image illustrates heterogeneous enhancement of mass with peripheral hyperintensity (consistent with vascular tumor) and central hypointensity (suggestive of necrosis).

C, Angiogram of left anterior descending artery shows that mass is perfused by septal perforator branch of left anterior descending artery and is highly vascular mobile tumor.

D, Intraoperative transesophageal echocardiogram obtained at time of resection and 3D reconstruction shows pedunculated round mass in right ventricle.

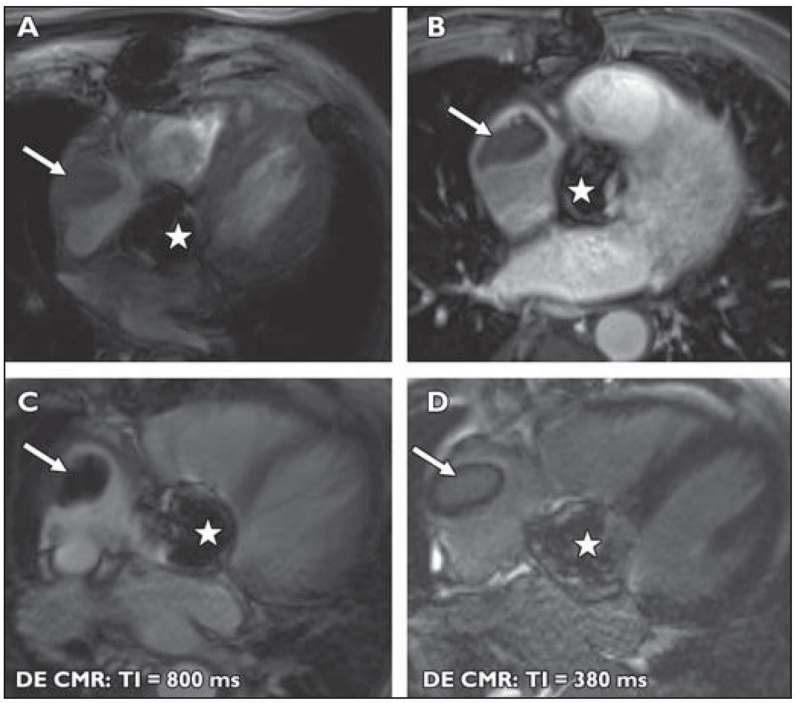

Fig 6. 76-year-old man with history of lymphoma and atrial fibrillation who was found to have right atrial mass on echocardiography. The patient had undergone aortic valve replacement 12 years previously

A–D, MR images show lobulated mass in right atrium (*arrow*) in this patient with atrial fibrillation and lymphoma. Susceptibility artifact is seen in region of prosthetic aortic valve (*star*). Mass does not enhance with IV contrast administration as seen on contrast-enhanced T1-weighted fat-saturation images (**A** and **B**). Ten minutes after administration of IV gadolinium, at inversion time of 800 milliseconds (**C**), mass becomes extremely hypointense. At inversion time of 300 milliseconds (**D**), myocardial signal is nulled and mass is isointense. Findings are consistent with right atrial thrombus.

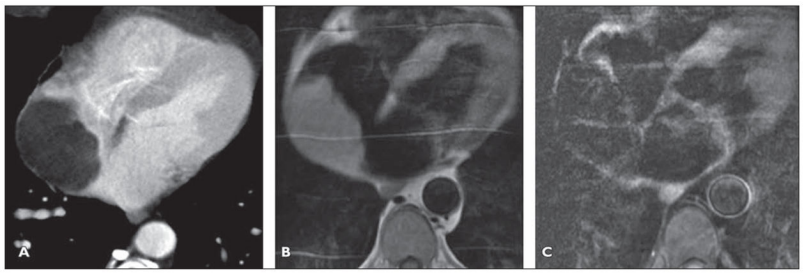

Fig 7. 60-year-old man who presented with near syncope

A, Contrast-enhanced CT image shows nonenhancing low-attenuation lipomatous mass (12 HU) within right atrium. Homogeneous attenuation, absence of solid elements, and absence of enhancement make liposarcoma unlikely. The Hounsfield units of this mass are consistent with fat, not thrombus.

B, T1-weighted four-chamber double inversion recovery image reveals mass is hyperintense.

C, After application of triple inversion to saturate fat signal, mass becomes hypointense.

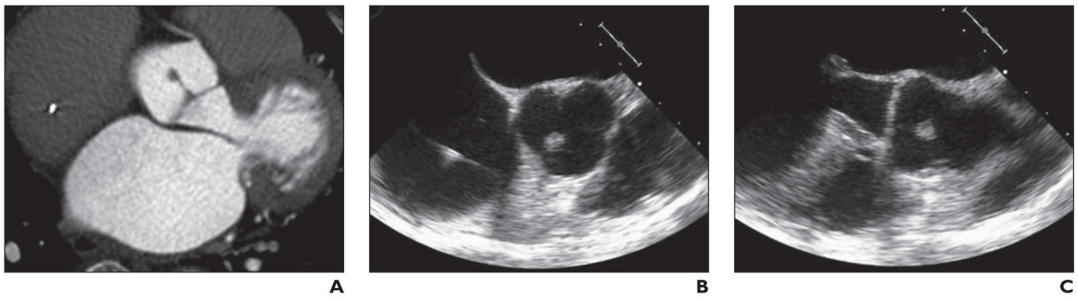

Fig 8. 77-year-old woman with shortness of breath on exertion who underwent echocardiography and was found to have mass adherent to aortic valve

A, Axial gated cardiac CT image shows 1-cm nodular excrescence arising from noncoronary cusp of aortic valve. On dynamic gated cardiac CT mass is seen to be mobile within aortic outflow tract and adherent to cusp by thin attachment (Figure S8A, cine loop, in supplemental data online). Contrast-enhanced gated dynamic cardiac CT was acquired using tube current modulation with reduced tube current output during retrospective data acquisition from full cardiac cycle; 75 mL of iopamidol (Isovue 370, Bracco) was administered at 6 mL/s followed by saline flush of 40 mL at 6 mL/s.

B and **C,** Cross-section images from transesophageal echocardiography of aortic valve (**B**) and left ventricular outflow tract and aortic root (**C**) show lobulated echogenic mass adherent to noncoronary cusp.

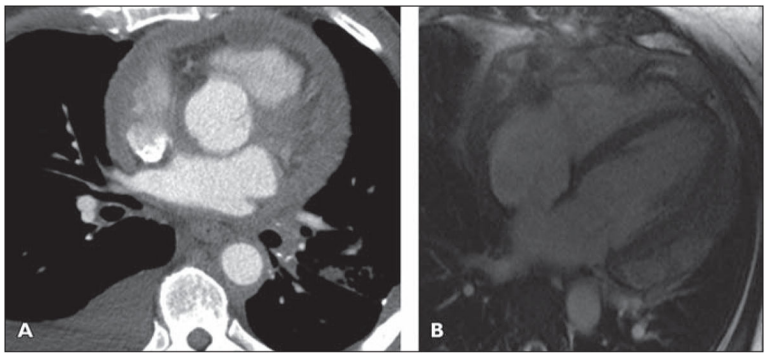

Fig 9. 47-year-old woman who presented with shortness of breath

A, Axial image from cardiac gated coronary CT angiogram after administration of 75 mL of nonionic contrast (370 mmol/mL) and 20 mL of saline flush all injected at 5 mL/s. There is circumferential thickening of pericardium and there appears to be well-maintained fat plane surrounding right coronary artery, but nodular and thickening pericardium more inferiorly in apical region encases and abuts distal left anterior descending coronary artery.

B, Four-chamber image from late gadolinium-enhanced cardiac MRI shows circumferential nodular enhancing pericardium. See also Figure S9B, cine loop, in supplemental data online.

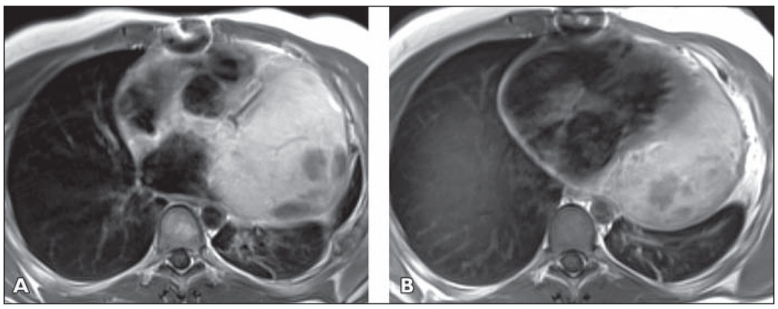

Fig 10. 23-year-old man with history of shortness of breath and back pain who was found to have pericardial mass biopsy-proven to be epithelioid mesothelioma

A and **B,** Axial T1-weighted double inversion recovery contrast-enhanced images show large heterogeneous mass extending from aorta to left hemidiaphragm, encasing right ventricular outflow tract, pulmonary artery, aortic root, and circumflex coronary artery. There is loss of epicardial fat in region of mid and distal anterior and anterolateral left ventricle, concerning for myocardial infiltration. See also Figures S10C and S10D, cine loops, in supplemental data online.

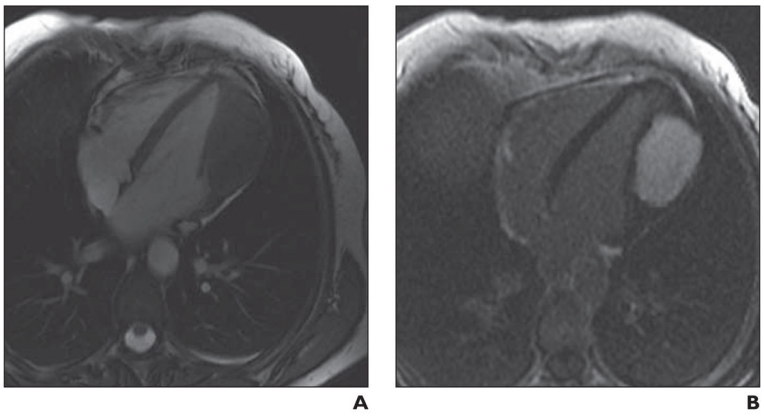

Fig 11. 42-year-old woman who presented with progressive shortness of breath and atypical chest pain

A, Four-chamber static image from fast imaging employing steady-state acquisition (FIESTA) sequence that has both T1 and T2 properties and is predominantly T2-weighted. Mass is seen in lateral wall of left ventricular myocardium. Mass is intramyocardial, and there is displacement of papillary apparatus within ventricle. Mass is predominantly isointense to muscle, with central areas of hypointensity consistent with predominantly fibrotic or necrotic tumor.

B, Delayed contrast-enhanced image (acquired 10 minutes after administration of weight-based dose of gadolinium) shows mass has diffuse homogeneous enhancement.

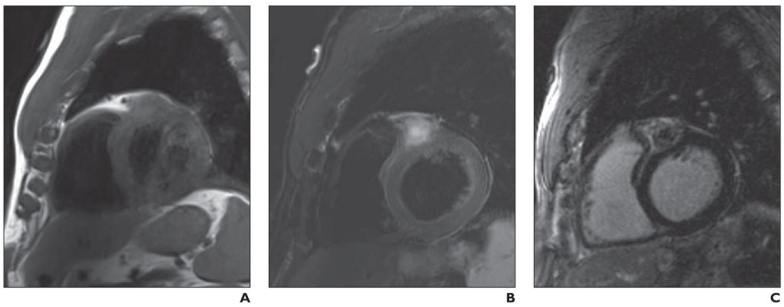

Fig 12. 69-year-old man with history of melanoma and incidental discovery of atrioventricular groove mass on echocardiography

A, Short-axis image from T1-weighted double inversion recovery sequence shows mass in right atrioventricular groove, which is mildly hyperintense relative to myocardium.

B, T2-weighted fat-saturation image shows high-intensity signal surrounding mass, consistent with edema.

C, After contrast administration (0.1 mmol/kg of gadolinium), there is enhancement of mass with central low intensity, consistent with central necrosis. Collectively, features are consistent with vascular tumor of atrioventricular groove. Mild T1 hyperintensity would be consistent with melanin in melanoma metastasis. Extent of melanin content of primary and secondary lesion will determine degree of T1 intensity.

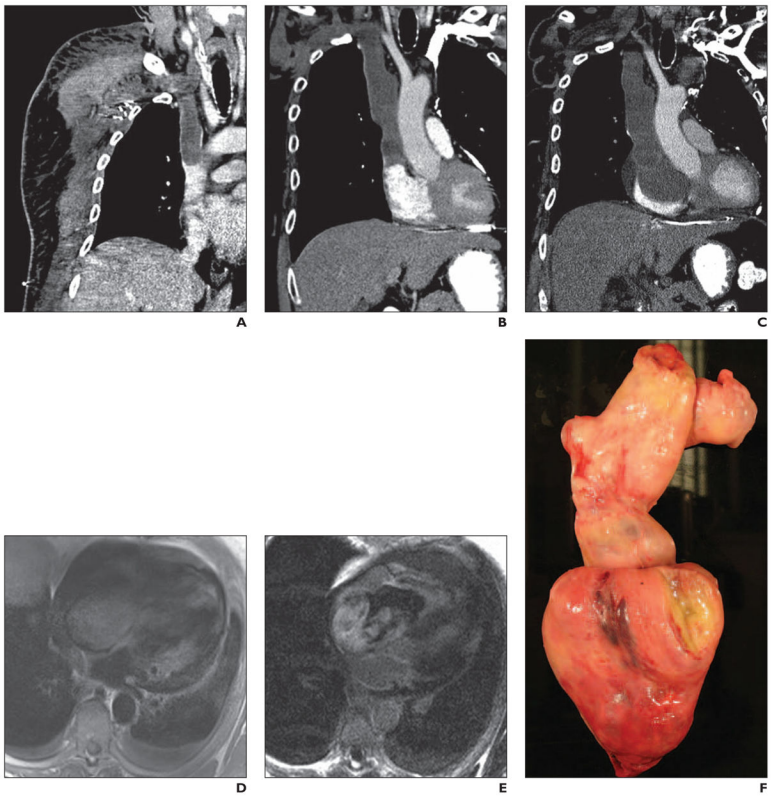

Fig 13. 65-year-old man who presented with mass and pain in right shoulder region found to be secondary to fibromyxoid sarcoma of scapula

A–C, Coronal images from contrast-enhanced chest CT show filling defect in superior vena cava (SVC) extending into heart. Patient has undergone right forequarter amputation.

D and **E,** Axial four-chamber image from T1-weighted sequence (**D**) and contrast-enhanced myocardial delayed enhancement image (**E**) at level of right atrium show large mass in right atrium and right ventricle, portion of which enhances whereas portion of mass does not, consistent with combination of tumor and thrombus.

F, Gross pathologic image shows mass excised from SVC and right heart (16.5 × 7.5 × 4.6 cm) that conforms to shape of SVC, right atrium, and right ventricle. Pathology was consistent with primary fibromyxoid tumor of right clavicle and confirmed transvenous extension of tumor.